

CONJUGATE PROBLEM OF HEAT EXCHANGE IN STEAM CONDENSATION
INSIDE A HORIZONTAL CYLINDER

V. M. Kapinos, L. A. Gura, and V. V. Navrotskii

UDC 536.423.4

The conjugate problem of heat exchange is solved for the case of condensation of slowly moving saturated steam in a horizontal tube without the formation of a draining stream in its lower part.

Many cases in technological practice often involve the problem of determining the heat-transfer coefficients and the general heat-transfer conditions in vapor condensation in horizontal tubes, in particular, in steam piping used for various purposes in atomic or thermal electric power plants under heating conditions. The nonuniformity along the periphery and along the wall thickness that arises in this case controls the heating rate and, thus, essentially, the pace of a certain part of the entire technological process.

The boundary conditions of heat exchange during condensation of stationary or slowly moving saturated steam in a horizontal pipe are usually determined by means of Nusselt's equations [1], derived for the isothermic outside surface of the pipe. Actually, the temperature distribution over the condensation surface is often nonuniform, which, as was shown in [2], markedly affects the local and the mean values of the heat-transfer coefficient. Since the temperature distributions inside the wall and at its surfaces are not known beforehand because they depend on the specific heat-exchange conditions, the use of Nusselt equations is difficult and fundamentally unjustified.

The interrelationship between condensation and the thermal conductivity of the wall is determined by solving the nonstationary conjugate problem that accounts for heat transfer by the condensate film, the storage capacity and the thermal conductivity of the metal wall, and the heat-exchange conditions at the outer bounding surface. The solution of the conjugate problem for a horizontal tube of infinite length is given below.

Film condensation of slowly moving saturated steam is contemplated under the assumption that the effect of surface tension forces is negligible. Moreover, it is assumed that the liquid running off into the lower part of the pipe does not form a stream at the bottom, but runs off through a conventional draining slot.

These assumptions allow us to consider the two-dimensional statement of the problem. The integration region (an arbitrarily chosen transverse cross section of the pipe) comprises two layers: the pipe wall, assigned by the inside R_1 and the outside R_2 radii, and the condensate film, whose thickness is determined in the process of solving the problem.

We use two coordinate systems with the common x axis, which is superposed on the inside surface of the tube, and the radial y axes, which are in opposition to each other. The coordinate origin is on the upper generatrix of the tube, in the symmetry plane. It is assumed that the thickness of the condensate film is much smaller than the curvature radius of the surface.

Variation of the film thickness along the periphery makes it difficult to use grid integration methods. Therefore, this region is reduced to the canonic — rectangular — form by passing to the relative radial coordinate $Y_1 = y_1/\delta(x)$. The present value of the condensate film thickness $\delta(x)$ is used as the transformation scale.

The other variables are reduced to dimensionless form by means of the following scale transformations: $X = x/R_1$; $U = u/\sqrt{gR_1}$; $V = v/\sqrt{gR_1}$; $T = t/t_s$; $\tau = \tau/M_s$; $Y_2 = y_2/\delta_w$. Different time scales are used, depending on the type of problem (nonstationary or stationary).

V. I. Lenin Kharkov Polytechnic Institute. Translated from *Inzhenerno-Fizicheskii Zhurnal*, Vol. 48, No. 3, pp. 495-502, March, 1985. Original article submitted December 23, 1983.

The initial system of equations, including the equations of motion (of the boundary-layer type), continuity, heat transfer, and thermal conductivity and the relationship between the mass and heat flows for determining the condensate film thickness are given by

$$\frac{\partial U}{\partial \tau} + U \frac{\partial U}{\partial X} + \left(\frac{R_1}{\delta_x} V - U \frac{Y_1}{\delta_x} \frac{d\delta_x}{dX} \right) \frac{\partial U}{\partial Y_1} = \left(1 - \frac{\rho''}{\rho'} \right) \sin X + \frac{v' \sqrt{R_1/g}}{\delta_x^2} \frac{\partial^2 U}{\partial X^2}, \quad (1)$$

$$\frac{R_1}{\delta_x} \frac{\partial V}{\partial Y_1} + \frac{\partial U}{\partial X} - \frac{Y_1}{\delta_x} \frac{d\delta_x}{dX} \frac{\partial U}{\partial Y_1} = 0, \quad (2)$$

$$\frac{\partial T}{\partial \tau} + U \frac{\partial T}{\partial X} + \left(\frac{R_1}{\delta_x} V - U \frac{Y_1}{\delta_x} \frac{d\delta_x}{dX} \right) \frac{\partial T}{\partial Y_1} = \frac{a_1 \sqrt{R_1/g}}{\delta_x^2} \frac{\partial^2 T}{\partial X^2}, \quad (3)$$

$$\frac{1}{M_\tau} \frac{\partial T}{\partial \tau} = \frac{a_2}{\delta_w^2} \left[\frac{\partial^2 T}{\partial Y_2^2} + \frac{1}{(R_1/\delta_w + Y_2)} \frac{\partial T}{\partial Y_2} + \frac{1}{(R_1/\delta_w + Y_2)} \frac{\partial^2 T}{\partial X^2} \right], \quad (4)$$

$$\frac{d\delta_x}{dX} \int_0^1 U \left[\frac{r}{t_s} + c_1(1-T) \right] dY_1 + \delta_x \frac{d}{dX} \int_0^1 U \left[\frac{r}{t_s} + c_1(1-T) \right] dY_1 - \frac{\lambda_1 \sqrt{R_1/g}}{\rho' \delta_x} \frac{\partial T}{\partial Y_1} = 0. \quad (5)$$

$$\text{For } X = 0 \text{ and } 0 < Y_1 < 1.0 \quad U = 0, \quad \frac{\partial T}{\partial X} = 0;$$

$$\frac{\partial \delta_x}{\partial X} = 0 \quad 0 \leq Y_2 \leq 1.0 \quad \frac{\partial T}{\partial X} = 0; \quad (6)$$

$$\text{for } X = \pi \text{ and } 0 \leq Y_1 < 1.0 \quad \left. \frac{\partial U}{\partial X} \right|_\pi = \left. \frac{\partial U}{\partial X} \right|_{\pi - \Delta X}, \quad \left. \frac{\partial T}{\partial X} \right|_\pi = \left. \frac{\partial T}{\partial X} \right|_{\pi - \Delta X};$$

$$0 \leq Y_2 < 1.0 \quad \left. \frac{\partial T}{\partial X} \right|_\pi = \left. \frac{\partial T}{\partial X} \right|_{\pi - \Delta X}; \quad (7)$$

$$\text{for } 0 \leq X \leq \pi \text{ and } Y_1 = 1.0 \quad U \frac{dG}{dX} = \frac{\mu_1 R_1}{\delta_x} \frac{\partial U}{\partial Y_1}, \quad V = \frac{\delta_x}{R_1} \int_0^1 \frac{\partial U}{\partial X} dY_1;$$

$$T = 1.0; \quad (8)$$

$$\text{for } 0 \leq X \leq \pi \text{ and } Y_1 = 0 \quad U = V = 0, \quad T_1 = T_2, \quad \frac{\lambda_1}{\delta_x} \frac{\partial T}{\partial Y_1} = \frac{\lambda_2}{\delta_w} \frac{\partial T}{\partial Y_2}; \quad (9)$$

$$\text{for } 0 \leq X \leq \pi \text{ and } Y_2 = 1.0 \quad \bar{\alpha}_{\text{coo}}(T - T_{\text{coo}}) = \frac{\lambda_2}{\delta_w} \frac{\partial T}{\partial Y_2}. \quad (10)$$

Equation (5) was obtained from the equation of thermal flux balance, written for an arbitrary film element with the thickness δ and the extent dx .

The boundary conditions (6) follow from the symmetry of condensate runoff over the pipe's inner surface. In the bottom part, the free-flowing condensate drainage is assigned as conservation of the rate of change in the sought functions (7). The slightly retarding action which the condensing steam mass exerts on the flowing liquid is reflected in the fact that the change in the momentum of this mass is equal to the friction stress at the interface between the phases (8). It is assumed here that the velocity of the condensed vapor mass increases from zero to the peripheral component value at the film surface. In accordance with the law of mass conservation in phase transition, the normal velocity component at the inter-

face between the phases is related to the increase in the condensate discharge along the X axis. The conditions of liquid adhesion and of ideal thermal contact between the liquid and the wall (9) are assigned at the inside surface of the pipe. The cooling conditions (10) on the outside are determined by the heat transfer coefficient and the coolant temperature.

The problem was solved by using the numerical method. On the time - space grid that we introduced, the differential equations were approximated by using the implicit, locally one-dimensional scheme of fractional steps. The calculation stability was ensured by "freezing" the coefficients in front of the convective terms of the equation of motion. The velocity derivatives were expressed in terms of their values at the adjacent grid nodes with the "floating" weight σ . For instance, the derivative of U with respect to X at the i-th node was approximated by means of the expression

$$\left. \frac{\partial U}{\partial X} \right|_i = \sigma \left. \frac{\partial U}{\partial X} \right|_{i-1} + (1 - \sigma) \left. \frac{\partial U}{\partial X} \right|_{i+1}.$$

Representation of the derivatives at the (i - 1)-th and the (i + 1)-th nodes by one-sided differences (with the error $O(\Delta X^2)$ in front and behind, respectively, makes it possible to obtain a three-point approximation of the first derivative in the following form:

$$\left. \frac{\partial U}{\partial X} \right|_i = \frac{(1 - 4\sigma)U_{i-1} - 4(1 - 2\sigma)U_i + (3 - 4\sigma)U_{i+1}}{2\Delta X}, \quad (11)$$

the error of which depends on the value of weight σ .

If $\sigma = 0.5$, expression (11) assumes the form of symmetric approximation of the derivative with the error $O(\Delta X^2)$. For all other σ values within the range from 0 to 1.0, the approximation error is equal to $O(\Delta X)$. The difference equations were solved by using the method of trial runs. The value of weight σ was determined from the condition of positive approximation ensuring calculation stability. If the sign in front of the derivative in the differential equation of motion or continuity is positive, then $\sigma < 0.25$; otherwise, $\sigma > 0.75$.

The use of three-point approximation is indispensable for derivatives with respect to the longitudinal coordinate and for the derivative of the sought transverse velocity component in the continuity equation.

Equation (5) was integrated by iterations with referral of the film thickness in the denominator of the third term to the preceding approximation. At the same time, condition (6) for the film was satisfied.

The conjugation of solutions of the energy and thermal conductivity equations was achieved by means of the generalized heat-exchange equation for the film-wall boundary surface. This boundary condition can be obtained from Eqs. (3) and (4) by putting $U = V = 0$ for $Y_2 = Y_1 = 0$. As a result, we obtain

$$\begin{aligned} \frac{\delta_x^2 c_1 \rho_1}{\sqrt{R_1/g}} \frac{\partial T}{\partial \tau} &= \left(\lambda_1 \left. \frac{\partial T}{\partial Y_1} \right|_m - \lambda_1 \left. \frac{\partial T}{\partial Y_1} \right|_{m-1/2} \right) / 0.5\Delta Y_1, \\ \frac{\delta_w^2 c_2 \rho_2}{M_\tau} \frac{\partial T}{\partial \tau} &= \left(\lambda_2 \left. \frac{\partial T}{\partial Y_2} \right|_{m+1/2} - \lambda_2 \left. \frac{\partial T}{\partial Y_2} \right|_m \right) / 0.5\Delta Y_2 + \frac{\lambda_2 \delta_w}{R_1} \left. \frac{\partial T}{\partial Y_2} \right|_m + \frac{\delta_w^2 \lambda_2}{R_1^2} \frac{\partial^2 T}{\partial X^2}. \end{aligned}$$

By summing the equations and considering the contact conditions (9), we obtain

$$A \frac{\partial T}{\partial \tau} = \frac{\lambda_2}{\delta_w} \left. \frac{\partial T}{\partial Y_2} \right|_{m+1/2} - \frac{\lambda_1}{\delta_x} \left. \frac{\partial T}{\partial Y_1} \right|_{m-1/2} + B \left. \frac{\partial T}{\partial Y_2} \right|_m + C \frac{\partial^2 T}{\partial X^2}, \quad (12)$$

where

$$A = \frac{\delta_x c_1 \rho_1 \Delta Y_1}{2\sqrt{R_1/g}} + \frac{\delta_w c_2 \rho_2 \Delta Y_2}{2M_\tau}; \quad B = \frac{\lambda_2 \Delta Y_2}{2R_1}; \quad C = \frac{\delta_w \lambda_2 \Delta Y_2}{2R_1^2}.$$

Equation (12) was approximated according to the general scheme. The temperatures at three grid nodes, (m - 1), m, and (M + 1), of which the middle one belongs to the layer bound-

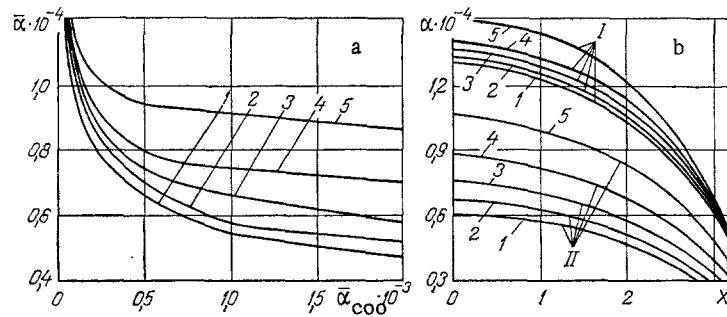


Fig. 1. Mean (a) and local (b) heat-transfer coefficients at the condensation surface as functions of the pipe wall thickness and the external cooling conditions ($t_{\text{coo}} = 20^\circ\text{C} = \text{const}$; I) $\bar{\alpha}_{\text{coo}} = 100$; II) $2000 \text{ W/m}^2 \cdot \text{K}$). 1) $\delta_w = 0.01 \text{ m}$; 2) 0.025 ; 3) 0.05 ; 4) 0.1 ; 5) 0.2 m .

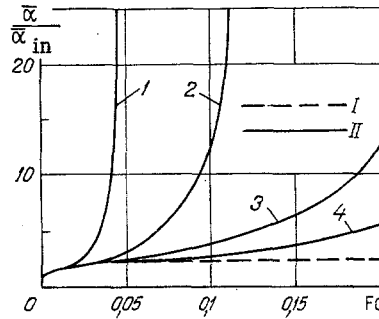


Fig. 2. Time variation of the relative heat-transfer coefficient in heating pipes by steam with constant parameters ($t_s = 150^\circ\text{C}$; (I) externally cooled pipe, $\delta_w = 0.1 \text{ m}$, $t_{\text{coo}} = 80^\circ\text{C}$, $\bar{\alpha}_{\text{coo}} = 300 \text{ W/m}^2 \cdot \text{K}$; (II) heat-insulated pipe, $t_o = 20^\circ\text{C}$). 1) $\beta = 1.086$; 2) 1.172 ; 3) 1.259 ; 4) 1.345 .

ary, were used along the Y axis. This made it possible to perform through trial runs in two layers in solving the difference equations.

The above approach involving conjugation of convective heat transfer and thermal conductivity was used in solving the stationary problem by means of the determination method. In the case of the nonstationary problem of heat exchange, conditions (9) were satisfied by successive approximations with separate solution of the equations describing the heat transfer in the film and in the wall.

In order to accelerate the calculation, the time scale M_τ was assumed to be equal to 1 h in solving the stationary problem; it was reduced to 72 sec in the case of the nonstationary problem in order to improve the accuracy of the intermediate results. The relative time interval was equal to 0.1.

The basic calculations were performed on a grid with 30 spacings along the X axis, 7 spacings along the film thickness, and 8 spacings along the wall thickness.

The initial conditions were used in the form of approximate film thickness, velocity, and temperature distributions.

The described method was checked by comparing the results of calculations of water vapor condensation on an isothermic wall with data obtained as a result of the Nusselt analytical solution [1]. The deviation of the mean heat-transfer coefficients did not exceed 1.5% in a wide range of parameter values. The results of calculations performed in the range of critical parameters $t_s = 370^\circ\text{C}$ for the temperature head $\Delta t = 90^\circ\text{C}$ are in good agreement with the conclusions reached in [3]. Consideration of the inertial forces and the convective heat transfer in the film for $K = 0.121$ and $\text{Pr} = 6.79$ leads to an increase by 52% in the mean heat-

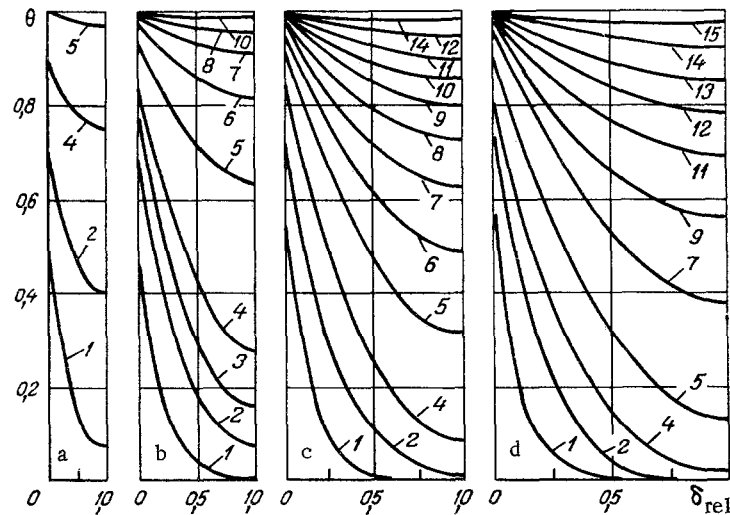


Fig. 3. Temperature profiles along the wall thickness in the region of the upper generatrix of heat-insulated pipes at different times [a) $\beta = 1.086$; b) 1.172; c) 1.259; d) 1.345]. 1) $Fo = 0.0011$; 2) 0.0043; 3) 0.0064; 4) 0.0096; 5) 0.021; 6) 0.032; 7) 0.043; 8) 0.054; 9) 0.064; 10) 0.075; 11) 0.086; 12) 0.107; 13) 0.128; 14) 0.161; 15) 0.214.

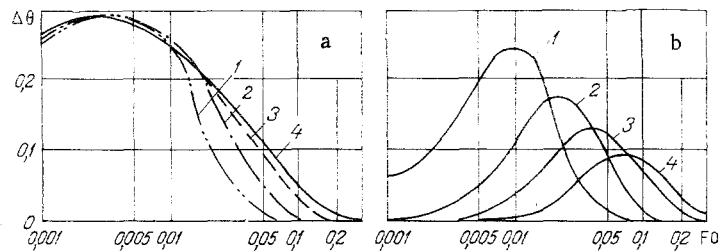


Fig. 4. "Top-bottom" temperature drop $\Delta\theta = \theta|_{x=0} - \theta|_{x=\pi}$ at the inside (a) and outside (b) surfaces of insulated pipes as a function of Fo . 1) $\beta = 1.086$; 2) 1.172; 3) 1.259; 4) 1.345.

transfer coefficient, or an increase by 49% according to data from [3], in comparison with the results obtained by means of the Nusselt equation.

Calculations of steady-state condensation conditions with an allowance for the thermal conductivity of the wall have shown that the temperature field of the pipe depends only on the radial coordinate over approximately two-thirds of its angular extent. Considerable axial asymmetry of the temperature field is observed in the bottom part of the pipe, where the thickness of the condensate film sharply increases. For equal condensation parameters and constant conditions of external cooling, the peripheral temperature nonuniformity increases with a reduction in the wall thickness. Thus, for $t_s = 150^\circ\text{C}$, $t_{\text{coo}} = 20^\circ\text{C}$ and $\bar{\alpha}_{\text{coo}} = 2000 \text{ W/m}^2\cdot\text{K}$ in a pipe with $R_1 = 0.29 \text{ m}$ and a wall thickness of 0.2 m, the "top-bottom" temperature drop amounts to 7°C , while, for a thickness of 0.01 m, it is equal to 33°C ($\lambda_2 = 45.4 \text{ W/m}\cdot\text{K}$).

As a result of the film thickening and the rise in the thermal resistance to condensation heat transfer with intensification of external cooling, the peripheral nonuniformity of the wall's temperature field increases. A change in $\bar{\alpha}_{\text{coo}}$ from 300 to $2000 \text{ W/m}^2\cdot\text{K}$ for a wall thickness of 0.01 m causes the temperature drop to increase from 10 to 33°C . An increase in the thermal conductivity of the wall also causes a rise in the temperature difference between the upper and lower generatrices of the two surfaces of the pipe. A change from 10 to $80 \text{ W/m}\cdot\text{K}$ in the value of λ_2 for a wall 0.01 mm thick produces an increase in these temperature drops from 21.7 to 34.5°C for $\bar{\alpha}_{\text{coo}} = 2000 \text{ W/m}^2\cdot\text{K}$. As the thermal conductivity coefficient increases, the effect due to the rise of the radial thermal flux is more pronounced than that due to the rise of the tangential flux. Therefore, the effects of λ_2 and $\bar{\alpha}_{\text{coo}}$ are qualitatively identical.

All other conditions being equal, an increase in the heat-transfer coefficient on the outside leads to a reduction in the mean heat-transfer coefficient at the condensation surface (Fig. 1a). This is caused by wall cooling, an increase in the vapor-wall temperature drop, and the thickening of the condensate film. However, a reduction in the heat-transfer coefficients does not indicate a lower condensation intensity; on the contrary, it indicates that this intensity increases. This apparent incongruity supports A. A. Mikhalevich's opinion [4] on the contradiction between the concept of the heat-transfer coefficient in condensation and its physical meaning. With a reduction in the wall thickness, the difference between the temperatures of its surfaces diminishes, which, for constant steam and coolant temperatures, produces an increase in the temperature head on the side of steam and a reduction in the heat-transfer coefficient in condensation.

The local values of the heat-transfer coefficient have a highly nonuniform distribution over the inside pipe surface if the overall level of these values is high (Fig. 1b). With an increase in the condensate film thickness, they are reduced by a factor of 3-4 in the lower part of the pipe.

The nonstationary problem of heating by steam with constant parameters was solved for cooled and heat-insulated pipes. In the first case, the increase in the heat-transfer coefficient during condensation (Fig. 2) is initially replaced by the asymptotic approach to values corresponding to the steady state at the end of heating. Its final value exceeds the initial one by a factor of 2.5. The maximum "top-bottom" temperature drop of 20°C that is initially established for $t_g = 150^\circ\text{C}$ and an initial wall temperature of 80°C gradually diminishes with a general equalization of the wall temperature.

The variation of the heat-transfer coefficient in an insulated pipe has a different character and is to a large extent determined by the wall thickness. The common feature characteristic for the different wall thicknesses is the gently sloping initial part of the $\bar{\alpha}(Fo)$ diagram and its steep rise due to the "drying-up" of the film at the final heating stage. The thicker the wall, the greater the extent of the gently sloping segment, which is explained by moderation of the wall temperature rise as a result of heat retention. After a 14-min interval following the start of heating of a pipe with $R_1 = 0.29$ m, the heat-transfer coefficient increases in comparison with its initial value by a factor of slightly more than 3 for the wall thickness $\delta_w = 0.1$ m, a factor of almost 5 for $\delta_w = 0.075$ m, and a factor of more than 18 for $\delta_w = 0.05$ m.

With a reduction in the wall thickness, the heating rate increases, and temperature equalization occurs faster in both the radial and the peripheral directions. Figure 3 shows the temperature distribution along the wall thickness in relation to β and Fo for $X = 0$. Comparing the four cases characterized by different wall thicknesses, we see that the heating time is reduced by one order of magnitude as β decreases from 1.345 to 1.086. Similar results were also obtained for the peripheral temperature distribution (Fig. 4). The greatest peripheral temperature nonuniformity develops initially at the heated surface and diminishes in the course of time (Fig. 4a). At the outside surface, the maximum temperature differences is the larger, the thinner the wall (Fig. 4b). The largest temperature differences develop later in time in pipes with a large wall thickness.

The above suggests that, because of the interrelationship between the condensation and thermal conductivity processes in pipe heating, the problem of determining the heat-transfer coefficients by means of Nusselt's equation is indeterminate, so that it must be solved as a conjugate problem. The temperature head between the wall and the condensing steam in this case varies both in time and along the longitudinal coordinate. At the same time, the local values of the heat-transfer coefficient are affected not only by the overall level of the temperature head, but also by the nonisothermicity of the wall and the longitudinal temperature gradient. It is impossible to separate in the conjugate problem the effect of the temperature gradient inside the wall in the direction of the condensate film flow; however, the calculations performed for an assigned nonisothermicity indicate that, for the power law of temperature variation $\bar{t} = (t - t_{\min}) / (t_{\max} - t_{\min}) = (1 - X)^n$, the mean heat-transfer coefficient diminishes by a factor of 1.3 as n increases from 0.25 to 4.

NOTATION

x, y , present coordinates; τ , time; X, Y , and \bar{t} , dimensionless space and time coordinates; δ_x , thickness of the condensate film; δ_w , thickness of the pipe wall; u and v , longitudinal and transverse velocity components, respectively; U and V , dimensionless velocity com-

ponents; t , temperature; t_s , saturated steam temperature; t_0 , initial wall temperature; Δt , temperature head; $\theta = (t - t_0)/(t_s - t_0)$, relative temperature of the pipe wall; T , dimensionless temperature; M_T , time scale; ρ , density; c , specific heat; λ , thermal conductivity coefficient; μ and ν , dynamic and kinematic viscosity, respectively; r , latent vaporization heat; g , acceleration due to gravity; α and $\bar{\alpha}$, local and mean heat-transfer coefficient, respectively; $a = \lambda/c\rho$, thermal diffusivity coefficient; $Pr = \nu/a$, Prandtl number; $Fo = a\tau/R_1$, Fourier number; $K = r/c\Delta t$, Kutateladze number; $\beta = R_2/R_1$, relative thickness of the pipe wall; dG , amount of condensate formed over the section dx ; ΔX and ΔY , discrete steps along the coordinate axes; i and m , grid node numbers. Subscripts: 1 and 2 pertain to the condensate film and the pipe wall, respectively; coo , coolant; $''$, vapor phase; $'$, liquid phase.

LITERATURE CITED

1. V. P. Isachenko, Heat Exchange during Condensation [in Russian], Énergiya, Moscow (1977).
2. D. A. Labuntsov, "Generalization of Nusselt's condensation theory encompassing the conditions of a spatially nonuniform temperature field of the heat-exchange surface," in: Heat Exchange and Hydraulic Resistance, Transactions of the Moscow Power Institute (Trudy MEI) [in Russian], Vol. 63 (1965), pp. 79-84.
3. D. A. Labuntsov, "Effect of convective heat transfer and inertial forces on the heat exchange in laminar condensate film flow," Teploenergetika, No. 12, 47-50 (1956).
4. A. A. Mikhalevich, Mathematical Simulation of Mass and Heat Transport in Condensation [in Russian], Nauka i Tekhnika, Minsk (1982).